Reconstruction of an ICESat Full Waveform by Terrestrial and Airborne Laser Scanning

K.H. Spaans and A.L.A.B. Ronse, Delft University of Technology

***Abstract*—Full Waveform Analysis using data obtained by the GLAS instrument onboard ICESat has been proven to be of great value in forest monitoring and land classification. This study looks at two other LIDAR measurement techniques, and assesses the possibilities in synthesizing the waveforms. While ICESat is a proven technique in forested areas, the number of groundtracks is limited, resulting in limited information. By looking at two more mobile and versatile techniques, a complimentary or even alternative method is hoped to be found.**

During this study, a forested area near IJmuiden is being considered. Data from the "Actueel Hoogtebestand Nederland" proved to contain insufficient information to reconstruct the waveform. Terrestrial laser scanning data however showed more promising results. By determining the height distribution in both data sets, a synthesized waveform was obtained. Due to difficulties in the registration process used, single scans had to be utilized in the TLS case. This meant an incomplete coverage of the ICESat footprint had to be considered, consequently leading to inconclusive final results. The results however do warrant further study.

***Index Terms*—ICESat, Full Waveform Analysis, Terrestrial Laser Scanning, Airborne Laser Scanning**

I. Introduction

LIGHT Imaging Detection and Ranging (LIDAR) is a remote sensing technique, which uses Light Amplification by the Stimulated Emission of Radiation (LASER) to measure the distance to an object. Nowadays its applications are already widespread, reaching from relatively cheap measuring devices to scanners, obtaining 3D images of their surroundings. The goal of this study is to determine the possibility of using two different LIDAR techniques to obtain the object height distribution in a forested area. These two techniques are terrestrial laser scanning (TLS) and airborne laser scanning (ALS). The obtained height distribution will be described in a waveform which is then compared with a spaceborne LIDAR technique already in frequent use over forested areas, the Geoscience Laser Altimeter System (GLAS) onboard ICESat. Possible applications, if successful, would be the determination of seasonal and annual variations within footprints.

The main problem in comparing the terrestrial laser scanner to the GLAS data lies in the difference in perspective. The GLAS signal reflects on the first surface it encounters, looking from the top. The GLAS data will therefore not reflect any underlying objects, contrary to the TLS data. If however the TLS data can be properly filtered to reflect only points that are visible from above, a relatively accurate reconstruction of the GLAS waveform should be possible.

To be able to reconstruct the ICESat full waveform using ALS, data from the "Actueel Hoogtebestand Nederland" (AHN) is used. This data does not have the perspective problem the TLS data has. It does however have relatively few measurements compared to TLS. The main problem will therefore be to determine whether the AHN data contain sufficient information on height distribution to be able to reconstruct the GLAS waveform.

The remainder of this article is composed of seven parts. Section II will briefly describe the three measurement techniques. The methodology used to obtain data, use it to reconstruct the waveform and compare it to the waveform is presented in sections III, IV, V and VI. Section VII contains the results, and finally in Section VIII, conclusion will be drawn.

II. Measurement techniques

All the data used in this case study were obtained using three instruments, based on LIDAR. These techniques will be briefly discussed in this part, starting with the GLAS instrument onboard ICESat. TLS and ALS will follow after that.

A. ICESat

The Ice, Cloud and land Elevation Satellite, or ICESat, is the first satellite used to make continuous observations of the Earth and its atmosphere using LIDAR. ICESat is in a near polar orbit at an altitude of 600 kilometers. The main component of ICESat is called GLAS.

The GLAS instrument is composed of the LIDAR instrument, a Global Position System (GPS) receiver and a star tracker. The LIDAR system contains three lasers, one of which broke down during the early testing phase [1]. Consequently, it was decided that the two remaining lasers would operate in discontinuous operational periods, in order to achieve the planned mission lifetime. These discontinuous operational periods have led to a decrease in the number of groundtracks over the Netherlands.

The lasers onboard GLAS send 4 ns pulses in the nadir direction at a pulse repetition frequency (PRF) of 40 Hz. On the groundtrack this leads to a footprint every 170 m. Every footprint has a diameter of approximately 70 m. The pulses are reflected from the ground, from objects, or even by the atmosphere and the reflected pulses are received by the telescope onboard ICESat. The travel time of the signal,

Karsten Spaans is a student at the Delft University of Technology, Faculty of Aerospace Engineering, Department of Earth Observation and Space Systems. Email: K.H.Spaans@student.tudelft.nl

Alexander Ronse is a student at the Delft University of Technology, Faculty of Aerospace Engineering, Department of Earth Observation and Space Systems. Email: A.L.A.B.Ronse@student.tudelft.nl

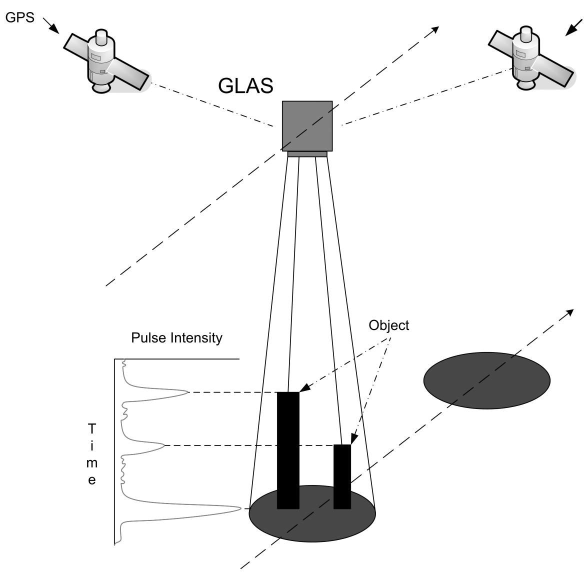

Fig. 1. Principal functioning of GLAS, showing how different parts of the footprint reflecting the signal create a waveform.

being measured by the satellites atomic clock, allows for the determination of the altitude:

$$h = \frac{c \cdot t}{2}, \tag{1}$$

where:

h	Altitude [m],
c	Speed of light [m/s], and
t	Two-way travel time [s].

To reference the altitude measurement, the GPS receiver and the star tracker determine the position and attitude of the satellite during each measurement.

The surface which reflects the laser signal is usually not a smooth surface, whether it is composed of water, ice, forestry or is an urban area. The signal therefore will be reflected at different altitudes and thus will be received by the GLAS at different times. The sampling frequency of the GLAS instrument is 1 ns, which means a precision of 15 cm in the range measurements. This sampling of the return signal creates a waveform, composed of the amount of energy received over time. From this waveform information can be obtained about terrain type, object heights and surface slope [2], which is known as full waveform analysis. Figure 1 shows the way GLAS functions.

B. Terrestrial Laser Scanning

TLS is a technique which utilizes laser signals to measure the range to an object. By combining the range with the direction of the signal, the position of that surface with respect to the scanner can be determined. If this process is repeated numerous times, a three dimensional point-cloud is created. In this study, the Faro LS 880 scanner is used [4].

To measure the range, there are three possible techniques, namely phase based, pulse based and triangulation. For this study, a phase based scanner was available, so this section will be limited to this technique. For a description of the pulse based and triangulation techniques, see [3].

Phase based range measurements determine the range by comparing the phase angle of the received (i.e. reflected) signal with the phase angle of a reference signal. If the wavelength of the signal is known, and two way travel of the signal is considered, the range to the reflecting surface can be determined using:

$$D = \frac{\alpha_{rec} - \alpha_{trans}}{2\pi} \cdot \frac{\lambda}{2}, \tag{2}$$

where:

D	Range to reflecting surface [m],
α_{rec}	Phase angle of received signal [rad],
α_{ref}	Phase angle of reference signal [rad],
λ	Wavelength of the laser signal [m].

Due to ambiguity, the maximum range of a phase based scanner is limited to half the wavelength of the laser signal [3]. A long wavelength signal is therefore needed. Precise determination of the phase angle of the long wavelength signal is however difficult, due to the slow variation over time of this phase angle. In order to counteract the precision problem in the FARO LS series scanners, the laser signal is tri-modulated with two shorter wavelengths, next to the long wavelength. The half-wavelengths used in the LS 880 scanner are 76, 9.6 and 1.2 meters [4].

Next to the range, the scanner has to record the direction from which the signal is received. By measuring the horizontal and vertical angle the signal makes with respect to the scanner, the direction is fully determined.

The output of the scanner is in Cartesian coordinates. The measurements however are in spherical coordinates (two angles and a range). A conversion from spherical to Cartesian coordinates must thus be made, using following relations:

$$x = R \cdot \sin\Phi \cos\theta, \tag{3}$$

$$y = R \cdot \sin\Phi \sin\theta, \tag{4}$$

$$z = R \cdot \cos\Phi, \tag{5}$$

where:

x, y, z	Cartesian coordinates of the measured point [m],
θ	Horizontal angle of the emitted signal [rad],
Φ	Vertical angle of the emitted signal [rad], and
R	Range between scanner and object [m].

Table I lists some specifications of the Faro LS 880 scanner, used in this study.

C. Airborne Laser Scanning

The third technique used in this study is ALS. A LIDAR device is mounted on an airplane or helicopter, which measures the range to the ground surface. Furthermore, GPS is used to determine the position of the aircraft at that instance in time. The Airborne Laser Scanning data used in this case study was provided by the AHN. The AHN is a database of surface altitudes over the Netherlands [5], and will be discussed at the end of this section.

In order to measure the range to an object, ALS uses a similar principle as ICESat, as described in Section II-A.

Ranging unit	
Range	0.6 - 76 m
Measurement speed	120,000 pps
Systematic distance error	3 mm at 25 m
Deflection unit	
Vertical field of view	320°
Horizontal field of view	360°
Vertical Resolution	0.009°
Horizontal Resolution	0.00076°
Maximum vertical scanning speed	1800 rpm
Laser	
Laserpower	20 mW
Wavelength	785 nm
Beam divergence	0.014°
Beam diameter	3 mm, circular

TABLE I
SPECIFICATIONS OF THE FARO LS 880. [4]

Pulses are sent towards the surface, and the two-way travel time is measured. ALS, however, does not acquire a waveform, but solely performs a first-last pulse measurement. The forward motion of the aircraft moves the LIDAR device towards its next measurement position, again similar to the ICESat mission. Accurate GPS measurements are needed as well to reference each range measurement. Contrary to the ICESat mission, ALS uses a side-sweeping motion of its laser to increase the number of measurements that can be done during one pass. The range measurement as done by an ALS system can thus be expressed as:

$$h = \frac{c \cdot t}{2} \cdot \cos\beta, \tag{6}$$

where:

h	Altitude [m],
c	Speed of light [m/s],
t	Two-way travel time [s],
β	Angle of signal with respect to nadir [rad].

Figure 2 shows the basic functioning of ALS.

As stated at the beginning of this section, the AHN is a database of surface altitude measurements over the Netherlands. It has a point density of at least 1 point per 16 m^2 area in the raw (unfiltered) data [6], which is the data used in this study. The data is given in meters, and positioning is done using the RD/NAP system. The RD/NAP system is an orthogonal system, and is the standard system used for geographical systems in the Netherlands. The y-axis runs from south to north, the x-axis from west to east. The origin lies near Paris, France, to ensure that all points in the Netherlands are made up of positive x and y coordinates. RD/NAP coordinates can be easily converted to latitude and longitude values using a coordinate calculator [7], which are used in the GLAS data.

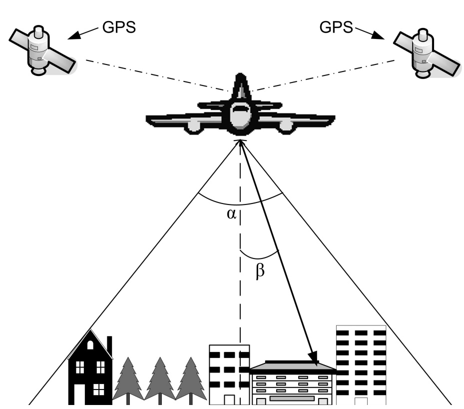

Fig. 2. Functioning of ALS, α represents the maximum scan angle, β the current scan angle.

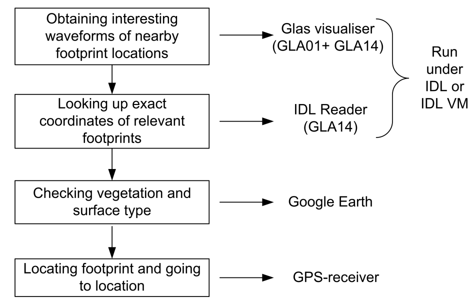

Fig. 3. Method sequence and used software for footprint determination

III. ICESAT DATA ACQUISITION AND CHOICE OF FOOTPRINT LOCATION

To ease processing, the GLAS data comes in the form of 15 convenient data products. For this study, the first (GLA01) and the fourteenth (GLA14) are used. GLA01 contains the global altimetry data, describing the raw waveforms and GLA14 contains the land altimetry data and exact footprint location, including range corrections. Upon request, both products can be acquired from the National Snow and Ice Data Center [8]. To reconstruct the ICESat waveform using TLS and ALS, a suitable footprint location is chosen. The method sequence and software which is used to do this, is described by Figure 3.

IV. TLS DATA ACQUISITION AND HANDLING

Once the footprint has been chosen, scans are made of it using the terrestrial laser scanner. The area is identified, and several scans are generated. The scan data are then filtered, registered and adapted to fit the needs of this study. Figure 4 shows the method used to obtain and handle the TLS data, which will be discussed in this section.

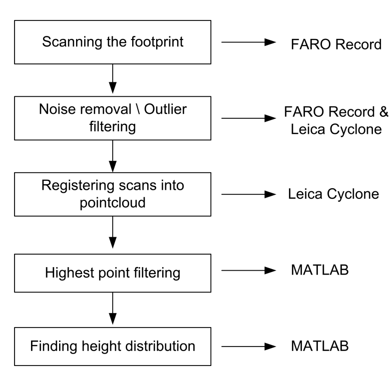

Fig. 4. Flow diagram of the TLS data acquisition and handling process, together with used software.

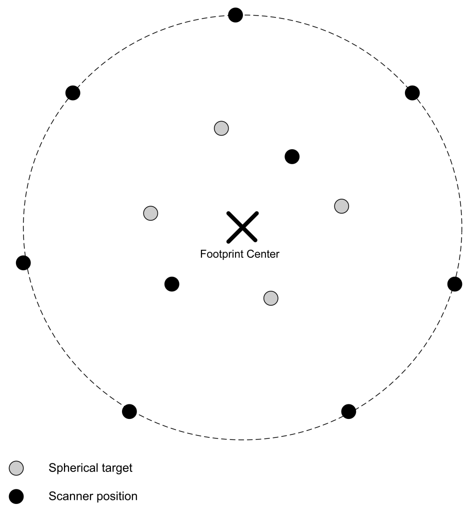

Fig. 5. Schematic representation of the scanning measurement setup

A. Scanning

Before the scanning can begin, the center of the footprint is located using GPS. Once the center point is known, the scan setup can be determined. Several scan positions, spread out in every direction, are marked at a distance of 20 m from the center. Planar targets are then fixed to trees, and four spherical targets are placed at points close by the center. For registration purposes, two center scan positions are added. A top view of the scan setup is given in Figure 5.

After the scan setup has been fully determined, the scanning itself can be carried out. It must be noted that the scan setup assumes the footprint of ICESat to be circular, where in reality it is slightly elliptical. Due to the uncertainty in GPS measurements (5-10 m) used to locate the center point, this assumption is reasonable.

B. Outlier filter

The raw scans recorded by the terrestrial laser scanner turned out quite noisy, as expected in a forested area. Several options were reviewed to remove this noise. The first and most obvious method is to manually remove the noise. The process of locating noise and subsequently removing it from the scan by hand is however very tedious, and especially in areas with many objects (trees, branches, bushes) not very effective. The outer edges of the scan can therefore be cleaned easily by hand, but the parts of the scan closer to the scanner are a bigger challenge.

To read the raw scan files made by the FARO LS, the programs FARO Record or FARO Scene are needed. These programs also come with several filter options. One of these filters is the outlier filter. For every point [9], the outlier filter compares the distance from the scanner to the point to the mean distance of all the points in a grid surrounding it. If the distance to the point under consideration deviates too much from the mean distance, the point is removed.

The filter mainly solves two big problems: it removes errors caused by a lack of reflections (scanning the sky), and it greatly reduces the noise in between branches, trees and other objects, caused by multipathing. After applying the filter, the outer edges of the scans still contain a large amount of noise. The filter does not work well on the outer edges, since the edges are mainly composed of noise. The mean distance of the scan points is therefore not influenced by objects at these points, and will thus less likely detect erroneous points. The noise at the edge of a scan can however be easily detected and removed manually.

C. Registration

After the outlier filter has been applied, the registration process is used to put all scans in one common coordinate system. This can be done using different methods and software. In this study, registration of the different scans is done by selecting points which are the same in two overlapping scans. The software which is used is *Leica Cyclone 5.8*, a program which visualizes point clouds and provides a series of work process options for laser scans.

To fully constrain two scans, a minimum of three common points has to be selected, but more can make the registration even more accurate. Constraining is also possible by selecting common 3D shapes or planes in two scans and constraining these. Using the method described above, registration is not done automatically -it works only by visually selecting common shapes or points- and is thus time consuming when the scans contain a lot of noise or contain insufficient reference points. It is thus desired to find a trade-off in resolution when scanning the area. Higher resolutions result in a lot of noise, while lower resolutions result in a lack of overlapping points.

D. Highest point filter

Two of the main problems when dealing with the TLS data are the large amount of data and the difference in perspective with respect to ICESat. In the process of handling the TLS data, a (partial) solution to both problems has been thought of. When comparing all the points with identical x and y coordinates, only the highest point of them should be considered. This greatly reduces the amount of points, and improves the compatibility of the TLS data set with the ICESat waveform with respect to perspective.

To create a filter performing the function as described above, MATLAB is used. To enable MATLAB to cope with such a large data set, it is split in 20 subsets. TLS data are given in meters, with 4 digits behind the comma, i.e. in tenths of a millimeter. In order to improve the number of points with identical horizontal coordinates, the data has to be put into a grid. The simplest method to do this is to round of the data. The choice was made to round of to the centimeter level. This value is a trade of between the reduction of points, computer power and the possible loss of height information.

Each subset of the original point cloud is then checked point by point. The maximum height for each grid point is found by comparing the z coordinate of every point to the current maximum value for the corresponding grid point. If the z coordinate is larger, this becomes the new current maximum. Figure 6 shows the results of the filter on a single tree, as well as the original data points. The shape of the original tree

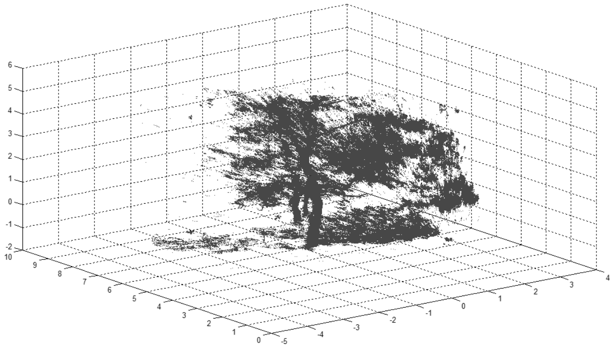

(a) Unfiltered tree

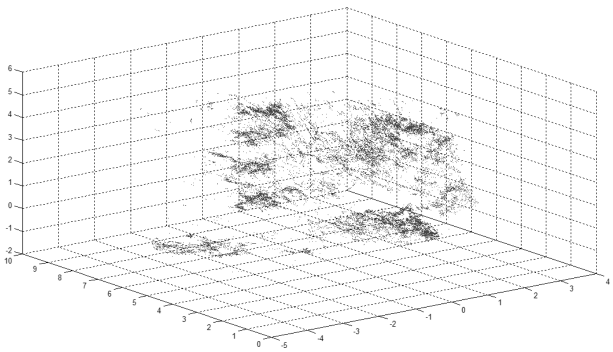

(b) Filtered tree

Fig. 6. Comparison between unfiltered and filtered data

remains identifiable in the filtered version, even though the number of points has been reduced from 950,000 to 22,000.

E. Height distribution

As a final step in the data processing, the height distribution has to be determined. This is done using a MATLAB program. The principal function of the program is simple: it first divides the total height into discrete height blocks, which are 17 cm high for the TLS scan. This height increment is determined by the program, and is related to the distance between the highest and lowest point, and the number of height blocks chosen. By counting how many points are contained in every height block, and storing this in an array, the height distribution can be used to synthesize a waveform. This synthesized waveform can be compared to the ICESat waveform.

V. AHN DATA ACQUISITION AND HANDLING

AHN data come in rectangular blocks of several kilometers width and length. The data come in ASCII-format, giving the RD x and y coordinates of a point, as well as the NAP height for that point. The data are filtered to reflect ground surface altitudes, thus for the purpose of this study the filtered out points have been obtained as well. By adding these points to the data, the point density is more than 1 point per 16 m^2. Figure 7 shows the steps which are taken in the acquisition and handling of the AHN data. The steps will be further discussed during this section.

A. Locating points

From the block of data points, only the points within the footprint scanned by ICESat are useful. If the footprint is assumed to be circular, all points within a range of 35 m of the center point are part of the footprint. The center point is first converted from longitude and latitude to RD-NAP coordinates. This is done using the coordinate calculator provided by RDNAP [7]. By subtracting the x and y coordinate of the center point from the x and y coordinates in the data set, the distance from the center to every point can be calculated easily with $D = \sqrt{x^2 + y^2}$, as shown by Figure 8. If the distance calculated is less than 35 m, the point is used for comparison.

B. Height distribution

To be able to make a comparison to the ICESat waveform, a similar process to the one described in Section IV-E for the TLS data is performed on the located AHN points. Roughly the same MATLAB code is used as with the TLS, with the exception that the height increment between different height blocks has been made a bit smaller. This to compensate for the lesser amount of data points available. A height increment of 10 cm was used.

VI. COMPARISON METHOD

When the height distribution waveforms of the AHN and TLS data are obtained, they can be visually compared to the ICESat waveform. However, a numerical comparison is desired to get more objective results. This is done by fitting a function, consisting of multiple Gaussian components to each waveform, a technique based on [2]. When this is done, the parameters of these Gaussians can be used for the numerical comparison. In this section, the steps which are used to get to the fitted functions are described.

A. Matching the data

In order to compare the synthesized waveforms to the original waveform, all need to be in the same order of magnitude, using the same parameters. The synthesized waveforms are composed of height distributions within a height element, while the GLAS waveform is given in bins based on the time the signal was received. The GLAS waveform data can however be converted to reflect height distributions, using eq. (1). The GLAS data bins are 1 ns apart, which equals 15 cm

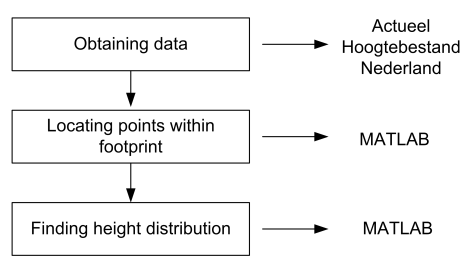

Fig. 7. Flow diagram of the ALS data acquisition and handling process, together with used software.

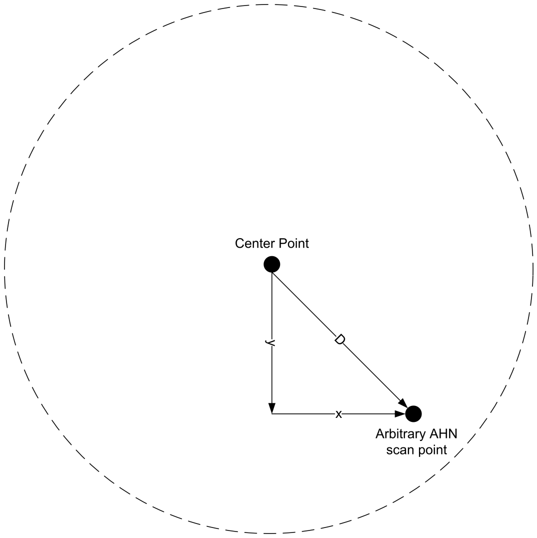

Fig. 8. Graphic representation of the program locating relevant AHN scan points

in height. It also has to be taken into account that the GLAS data gives the height distribution from the highest point to the lowest point, while the synthesized waveforms give the height distribution from the lowest point to the highest point. Therefore the order of the bins of either the original waveform or the synthesized waveforms have to be reversed. The choice is made to reverse the GLAS data.

The simplest method to get all the height distributions in the same order of magnitude is to normalize the data, taking into account the number of bins. The GLAS waveform is normalized by dividing the received energy at point i, V_i, by the total energy, V_T. The total energy is defined as $\sum_{i=1}^{N} V_i$, where N is the total number of points. The same method is used for the TLS and AHN synthesized waveforms, with an additional scaling factor. This scaling factor is introduced to compensate for the difference in the number of data bins of the different waveforms, and is defined as the ratio between the number of bins of GLAS (N_{GLAS}) and the number of bins of the synthesized waveform (N_{synth}), $SF = \frac{N_{GLAS}}{N_{Synth}}$. The complete normalization process is therefore described by:

$$V_N(i) = \frac{V_i}{V_T} \cdot SF. \qquad (7)$$

The last step in matching the data is finding a common point, with respect to which the relative height distributions can be compared. The common point is the maximum value of the first mode[1] of the waveforms. It is assumed that the first modes all represent the mean ground level, and this point is set to height zero, thus enabling the synthesized waveforms to be plotted with the original waveform.

[1]In Full Waveform Analysis (FWA), peaks in the waveforms are labeled modes. Due to the reversed order of the bins, the ground in the GLAS waveform is represented by the last mode. To avoid confusion however, in this paper the mode representing the ground will be called the first mode.

B. Fitting algorithm

In this step, Gaussian components are fitted to the normalized waveforms. It is thus assumed that each waveform $w(h)$ roughly consists of a sum of Gaussian components W_m:

$$w(h) = \sum_{m-1}^{N_p} W_m(h), \text{ with } \quad W_m(h) = A_m e^{\frac{-(h-h_m)^2}{2\sigma_m^2}} \qquad (8)$$

where:

$w(h)$	Fitted waveform at height h,
$W_m(h)$	Fitted Gaussian component at height h,
N_p	Number of Gaussians,
A_m	Amplitude of Gaussian m,
h_m	Center position of Gaussian m [m],
σ_m	Standard deviation of Gaussian m [m].

After a visual estimation of each Gaussian's location in the waveform, the least squares approach is used to fit the components and determine the amplitude, center position and standard deviation of each of them. This can be done using MATLAB.

C. Numerical comparison

Using the parameters obtained by the Gaussian fitting, a numerical comparison can be made between the resulting waveforms. To do this, one has to select corresponding Gaussian components in all waveforms. Different parameters which can be compared to each other are:

- Gaussian center position
- Gaussian standard deviation
- Gaussian amplitude
- Gaussian slope
- Waveform extent (distance between first and last Gaussian)

VII. Results

In this chapter, the methodology described in the previous sections is applied to a chosen ICEsat footprint. The relevant TLS and AHN data of the location are obtained, processed and converted to height distribution waveforms and finally compared to the ICESat waveform.

A. Footprint and raw waveform

A footprint just south of IJmuiden was chosen, as the terrain there is forested and the waveform contains interesting aspects. An image describing the ground track and footprint location is shown in Figure 9. The raw received waveform, shot at the 30th of September 2003, is depicted in Figure 10.

B. TLS waveform comparison

For this study, two series of scans of the footprint were made; the first scans were made at 1/4th of the maximum resolution of the scanner, see Table I. This resolution led to a large amount of noise and thus a time consuming registration process. Furthermore, the first set of scans did not contain enough artificial targets, thus further complicating the registration process. The combined effect of the noise and the lack

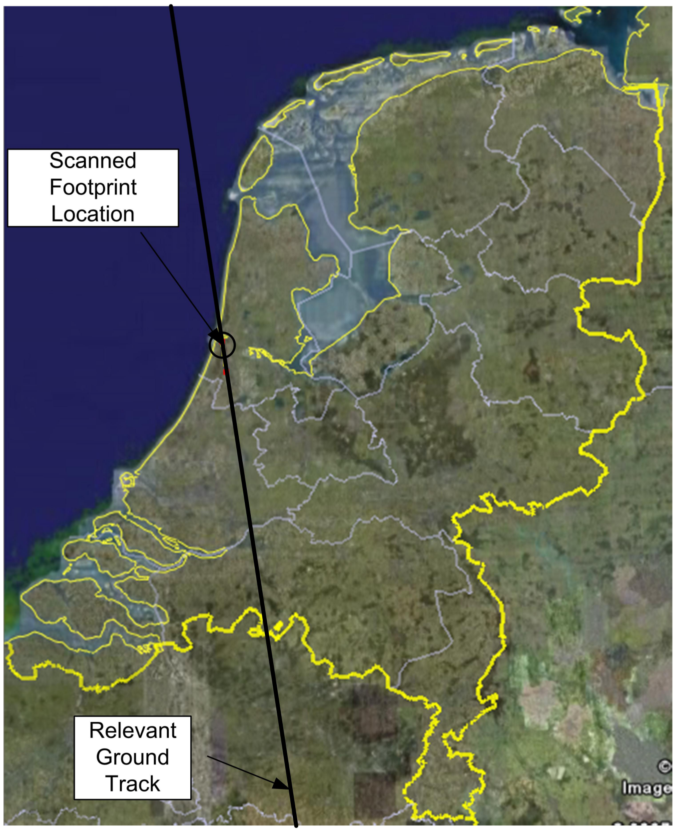

(a) Relevant ICESat ground track and chosen footprint location

(b) Zoomed picture of chosen footprint

Fig. 9. Images of footprint location. [10]

of targets made registration impossible using the traditional approach.

The second series were made using 1/10th of the maximum resolution. This led to faster scanning, but the process also required more targets, as the maximum scan distance reduces when the resolution gets lower. Sadly, 3 out of 8 scans in this set were lost due to corruption of the data. Due to the fact that the lost scans were essential to the registration process, because of their relative location with respect to the other

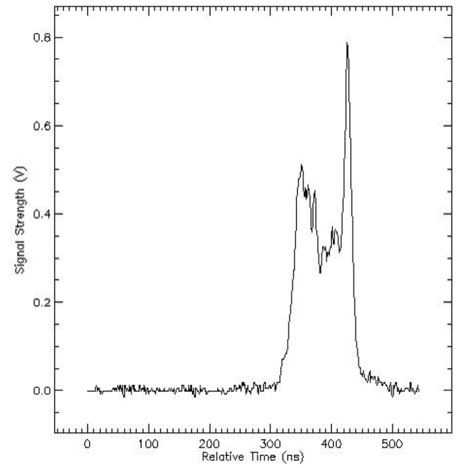

Fig. 10. Raw waveform of chosen footprint

scans, registration again failed [2]. The remainder of this section will utilize two single scans of the first set. The choice to use scans from the first set was made due to the higher resolution. The higher resolution scans contain a larger area, since they can distinguish different objects at larger ranges. Less scan points on the outer edge of the scan have to be removed, leaving a radius of approximately 25 m. The radius of the low resolution scans after cleaning is less than 20 m. A further advantage of the first set of scans is that they were obtained at the same seasonal period as the original footprint, leading to similar conditions concerning the amount of leafs on the trees. The two scans used for the comparison are called scan A and scan B for the remainder of this paper. Scan A was made in an area where most of the tallest trees were located. The scanner position in scan A was not situated at the center of the footprint, however it is assumed that the majority of filtered points are within the ICESat footprint. Scan B was obtained in the center of the footprint. Yet, this area contained lesser trees in close proximity to the scanner.

Normalizing the obtained height distributions leads to a first (visual) comparison to the normalized ICESat waveform. The normalized waveforms of scan A and B, together with the normalized ICESat waveform, are depicted respectively in Figure 11(a) and 11(b).

Next, multiple Gaussian components are fitted to both waveforms, leading to a numerical comparison of some of the waveform parameters. As scan A is the one which contained most of the large features of the footprint, this is the one which corresponds most closely to the ICESat waveform. In Figure 12 the normalized waveform of scan A and the ICESat normalized waveform are depicted together with the fitted waveform and the three Gaussian components. As can be seen, the fitted waveforms are alike. It can be noticed that the first peak (ground peak) is higher and thinner in the TLS case. This is due to the fact that the TLS data come from one single scan, which means the ground level does not vary as much within the

[2]Regarding to future registrations of scans in forested areas, a scan resolution of 1/5th or 1/8th, together with a redundant amount of targets and spheres is recommended. Other registration techniques might also lead to better results.

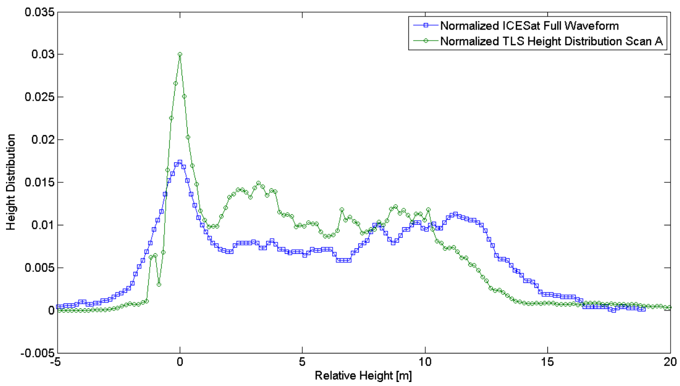

(a) Synthesized waveform using scan A

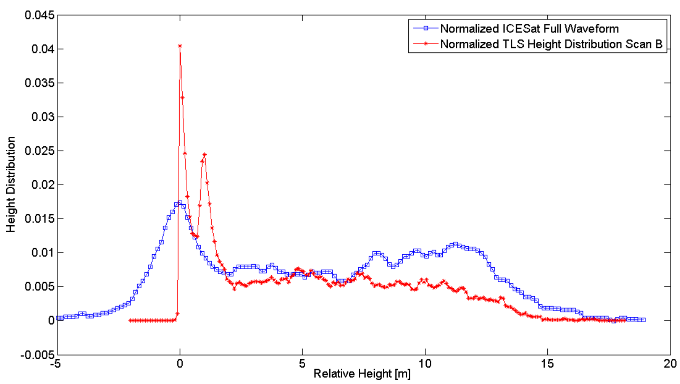

(b) Synthesized waveform using scan B

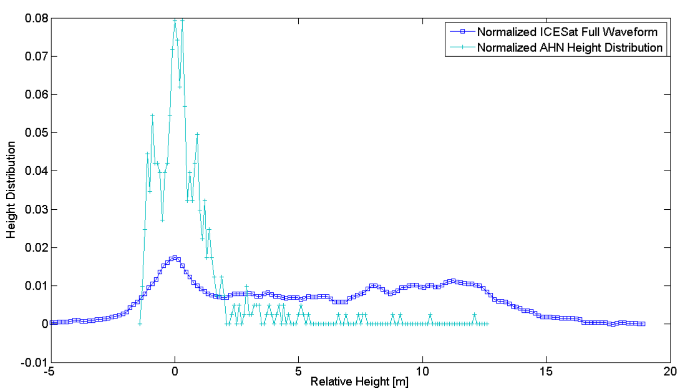

(c) Synthesized waveform using AHN

Fig. 11. Three synthesized waveforms compared to the original

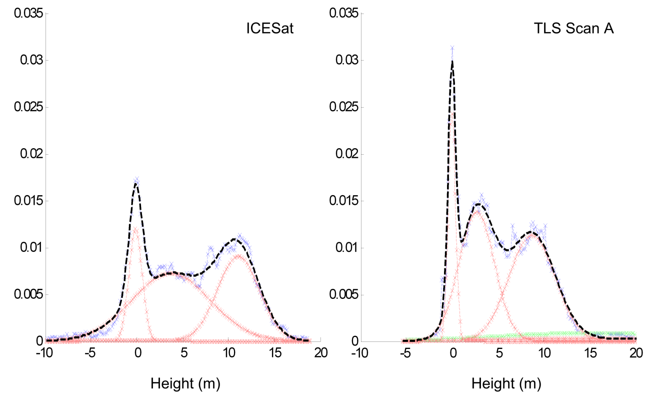

Fig. 12. TLS and ICESat fitted waveforms (black),normalized waveforms (blue) and Gaussian components (red).

scanned area as it does within the entire footprint. This makes the peak thinner in the TLS waveform. When normalizing the waveform, the area below the graph has to be unity, resulting in a higher peak than in the ICESat case. Furthermore, one can see that the middle lobe is higher in the TLS waveform. An explanation for this fact may be that the TLS also scans the trunks and branches which are underneath the canopy of the trees. Some of these are not filtered out. ICESat, however, cannot detect all these objects, as the canopy partially blocks its view.

It has to be stressed that the TLS waveform in the figure is the result of only one scan, and thus not representative for the whole footprint. If one wants more reliable results, a registered point cloud should be used, consisting of multiple scans. For the sake of demonstrating the process, two TLS scans will now be numerically compared to the ICESat waveform, from which some preliminary conclusions can be drawn.

In one TLS scan used for the comparison (scan A), the obtained waveform was closely enough related to the ICESat waveform to select three corresponding Gaussians in both data sets, see Figure 12. For the other TLS scan (scan B), only two Gaussian components are estimated, being the ground peak and the more stretched and lower amplitude waveform after it. This fit is then compared to a two-component estimation of the ICESat waveform. The three-component comparison between scan A and ICESat can be seen in Table II and the two-component comparison between scan B and ICESat in Table III.

Looking at the three-component case, it is seen that the peak center location parameter of each Gaussian is relatively comparable. The peak-locations do not differ more than 2.3 meters from one another. The standard deviations and amplitude, on

		Gaussian STD [m]	Gaussian mean [m]	Gaussian Amplitude[-]
Peak 1:	TLS Scan A	0.4003	-0.0359	0.0244
	ICESat	0.7222	-0.1343	0.0120
Peak 2:	TLS Scan A	1.9480	2.6729	0.0138
	ICESat	4.2641	3.7296	0.0072
Peak 3:	TLS Scan A	2.5217	8.7158	0.0113
	ICESat	2.2830	11.0838	0.0090

TABLE II
PARAMETER COMPARISON BETWEEN SCAN A WAVEFORM AND ICESAT WAVEFORM.

		Gaussian STD [m]	Gaussian mean [m]	Gaussian Amplitude[-]
Peak 1:	TLS Scan B	0.6213	0.6315	0.0191
	ICESat	0.8659	-0.0893	0.0132
Peak 2:	TLS Scan A	4.4653	6.6201	0.0069
	ICESat	5.3927	7.9275	0.0093

TABLE III
PARAMETER COMPARISON BETWEEN SCAN B WAVEFORM AND ICESAT WAVEFORM.

the other hand, do vary. As already explained, this probably has to do with the fact that the TLS waveform represents a smaller area.

As the scan B waveform shows less similarity with the ICESat waveform, a very general function consisting of two Gaussian components is used. One Gaussian represents the ground peak, the other one the remainder of the waveform, thus the whole set of objects above the ground. This however, results in a great loss of details about the forrest features. A three-component fit would be useless, as no relation can be found between other peaks than the ground peak. Observing the comparison parameters, one can see that all parameters do not differ largely. The second Gaussian components are, however, very general and not really detailed fits.

Again, for a much more reliable comparison between the TLS waveform and the ICESat waveform, one is advised to use a registered point cloud. The single scans used here are only examples of how the comparison is made. Nevertheless, the methodology for the comparison would be exactly the same for the registered point cloud.

C. AHN waveform comparison

Using the methodology described in section V and VI, the normalized and AHN height distribution waveform is obtained and compared to the ICESat waveform. The AHN waveform laid over the ICESat waveform is seen in Figure 11(c). The AHN data within the waveform contain only 503 points. Furthermore, the AHN is actually made to only measure the ground surface height throughout the Netherlands. These two facts combined explain why the AHN waveform does not resemble the ICESat waveform much. One can however also distinguish a ground peak and some points at higher altitudes. The position of the last points is also near the canopy top of the ICESat waveform, which shows the waveform extent is also more or less similar. Due to the very low point number, it was considered irrelevant to fit any Gaussian components and do a numerical comparison between the two waveforms.

VIII. Conclusion and Recommendations

Throughout this study, methodology for synthesizing an ICESat waveform using TLS and AHN data was developed and tested. The synthesizing methodology for TLS data consisted of filtering, registering, determining height distribution and normalizing in order to be able to compare it to the ICESat waveform. The data which was then used for the testing, consisted of two separate scans instead of a registered point cloud due to problems in the registration process. Relations could be seen between both data sets, especially in one of the two scans. All Gaussian components were situated at more or less the same locations within the waveform. The discrepancies in the other Gaussian parameters could possibly be explained by the fact that the separate laser scans did not contain the whole footprint area. For the AHN data, the methodology comprised locating relevant data points and determining the height distribution. The data do not contain many points within the footprint and thus the height information is rather limited when compared to the ICESat and TLS data. A ground peak could be observed and the extent was similar, but no necessity was seen in fitting Gaussian components.

The main recommendation with respect to waveform reconstruction using TLS, is the use of a registered point cloud to compare the TLS data. In this study only separate scans were used, just as an example of how the methodology is applied. For a more reliable comparison, a registered point cloud covering the entire footprint is to be used. Only one approach to registering separate scans into a point cloud was reviewed during this study, however other techniques are available. These alternative techniques might lead to better results regarding registration.

It is also advised to attempt to validate the developed techniques over several footprints. Due to time constraints, this study was limited to footprints within a certain area. This excluded interesting areas like the Ardennes in Belgium or the Eiffel region in Germany. These areas contain much larger forests, and are thus interesting areas to test the TLS synthesizing technique.

A further advantage of expanding the area of interest is the availability of more recent footprints. The footprint chosen in this study was from the fall of 2003, which meant 4 years had already passed when the TLS scan was obtained. A more recent footprint limits the probability that the footprint area undergoes major changes.

Acknowledgment

The authors would like to thank Sylvie Soudarissanane, MSc and Hieu Van Duong, MEng for the guidance, patience and expertise provided continuously during this study. Furthermore the authors would like to thank Dr. R.C. Lindenbergh and Dr. R.F. Hanssen for their help reviewing the paper and giving general feedback on the study.

References

[1] National Aeronautics and Space Agency, *ICESat official website*, http://icesat.gsfc.nasa.gov/, Last visited: October 2007

[2] H.V. Duong, N. Pfeifer, R.C. Lindenbergh, *Analysis of repeated icesat full waveform data: Methodology and leaf-on leaf-off comparison.*, In proceedings: Workshop on 3D Remote Sensing in Forestry, Vienna, 2006.

[3] J. M. van Ree, *Determination of the precision and reliability parameters of terrestrial laser scanners.*, Masters thesis, Delft University of Technology, 2006.

[4] FARO Technologies Inc., *FARO Laser scanner LS Brochure*, August 2005

[5] Actueel Hoogtebestand Nederland, *Actueel Hoogtebestand Nederland official website*, http://www.ahn.nl, Last visited: December 2007

[6] R. M. van Heerd et al., *AHN Productspecificatie*, Technical report, Rijkswaterstaat i.c.w. Adviesdienst Geo-informatie en ICT, 2000

[7] RD-NAP, *RD-NAP website*, http://www.rdnap.nl, Last visited: December 2007

[8] National Snow and Ice Data Center, *NSIDC website*, http://nsidc.org/data/icesat, Last visited: December 2007

[9] FARO Technologies Inc., *FARO Scene 3.0 User's Manual*, Product manual, 2005

[10] Google, *Google Earth*, http://earth.google.com/intl/nl/, Last visited: December 2007